

# Effect of different arch widths on the accuracy of three intraoral scanners

Narin Kaewbuasa, Chakree Ongthiemsak\*

Department of Prosthetic Dentistry, Faculty of Dentistry, Prince of Songkla University, Hat Yai, Songkhla, Thailand

## ORCID

Narin Kaewbuasa

<https://orcid.org/0000-0002-8286-4624>

Chakree Ongthiemsak

<https://orcid.org/0000-0001-7013-204X>

**PURPOSE.** The purpose of this study was to compare the accuracy of three intraoral scanner (IOS) systems with three different dental arch widths. **MATERIALS AND METHODS.** Three dental models with different intermolar widths (small, medium, and large) were attached to metal bars of different lengths (30, 40, and 50 mm). The bars were measured with a coordinate measuring machine and used as references. Three IOSs were compared: TRIOS 3 (TRI), True Definition (TD), and Dental Wings (DW). The relative length and angular deviation of both ends of the metal bars from the scan data set ( $n = 15$ ) were calculated and analyzed. **RESULTS.** Comparing among scanners in terms of trueness, the relative length deviation of DW in the small (1.28%) and medium (1.08%) arches were significantly higher than TRI (0.46% and 0.48%) and TD (0.33% and 0.18%). The angular deviation of DW in the small (1.75°) and medium (1.83°) arches were also significantly greater than TRI (0.63° and 0.40°) and TD (0.55° and 0.89°). Comparing within scanner, the large arch of DW showed better accuracy than other arch sizes ( $P < .05$ ). On the other hand, the larger arch of TD presented a greater tendency of angular deviation in terms of trueness. No significant differences were found in terms of trueness between the arch widths of TRI group. **CONCLUSION.** The different widths of the dental arches can affect the accuracy of some intraoral scanners in full arch scan. [J Adv Prosthodont 2021;13:205-15]

## KEYWORDS

Intraoral scanner; Accuracy; Digital impression; Arch width; Arch size

## Corresponding author

Chakree Ongthiemsak  
Department of Prosthetic  
Dentistry, Faculty of Dentistry,  
Prince of Songkla University  
15 Kanjanavanich road, Hat Yai  
District, Songkhla 90112, Thailand  
Tel +6674429874  
E-mail [chakree.o@psu.ac.th](mailto:chakree.o@psu.ac.th)

Received June 15, 2021 /  
Last Revision August 5, 2021 /  
Accepted August 9, 2021

This study was supported by a research grant from the Royal College of Dental Surgeons of Thailand, and Department of Prosthetic Dentistry, Prince of Songkla University.

## INTRODUCTION

Digital dental impressions by an intraoral scanner (IOS) are increasingly used today. There are many benefits of using an IOS over a conventional impression, such as not touching the oral tissue, no potential choking hazards, the immediate display of the impression details on the screen, and time-saving.<sup>1,2</sup> Many IOSs in the market today use different technologies to deter-

© 2021 The Korean Academy of Prosthodontics

© This is an Open Access article distributed under the terms of the Creative Commons Attribution Non-Commercial License (<http://creativecommons.org/licenses/by-nc/4.0>) which permits unrestricted non-commercial use, distribution, and reproduction in any medium, provided the original work is properly cited.

mine distance to object (confocal microscopy, active wavefront sampling, active triangulation, and optical coherence tomography) and different acquisition methods (individual image and video sequence).<sup>1,3,4</sup> Furthermore, various studies over the past few years have found that scanners with different technologies offer different accuracy of the scanned files.<sup>4-7</sup> The accuracy of the dental impression affects the quality of the restoration, and the poor marginal adaptation of a dental prosthesis can cause secondary caries or periodontal disease. However, there is still some controversy about the accuracy of IOSs, and the studies have shown conflicting results.<sup>4,7-13</sup>

The term 'accuracy' infers trueness and precision. Trueness is defined as the ability of a measurement to match the actual value. Precision refers to the ability of a measurement to be consistently repeated.<sup>14</sup> Two methods are generally used to measure the trueness of the scanner. One method is to superimpose the scanned file with a reference data set from a high accurate scanner. The other method is used for measuring the distance, angle, or size of the geometric object that is attached to the dental arch and compares the measured values with the reference value obtained from a highly accurate measuring instrument. Different shapes of the precise objects can be used, such as a metal sphere, metal bar, or gauge block.<sup>15-17</sup> A coordinate measuring machine (CMM) is a highly accurate device that has often been used to measure the geometry of those objects.

In addition, computer-aided design (CAD) and computer-aided manufacturing (CAM) have provided sufficient clinical marginal and internal fits for a single unit and the same quadrant restorations. However, in case of full arch scanning, they have also shown more deviations and less accuracy than the traditional process.<sup>11,18-20</sup> As IOS is unable to capture the dental arch with a single scan, multiple scan images have to be taken and stitched together at overlapping areas to obtain the oral structures. Previous studies have also shown that the scan distance affected the accuracy of the scanners, where the deviation increased with the extended length of the scan section, and the greatest discrepancy occurred in the second molar area.<sup>14,21</sup> However, those studies reported deviations at each position of the same arch, while there have been very

few comparisons of the studies of different arch sizes. Only one study compared the accuracy between the different dental arch widths and reported that the arch width did not affect the trueness of the IOS.<sup>22</sup> Therefore, additional information is needed on this topic.

The purpose of this *in vitro* study was to evaluate and compare the accuracy of three IOSs with three different dental arch widths. The null hypotheses were that no difference would be found in the accuracy (trueness and precision) of the scan from the three IOSs within the same arch width and that no difference would be found in the accuracy of the scan from the three dental arch widths when the scan data sets were compared within the scanner.

## MATERIALS AND METHODS

Three different lengths (30, 40, and 50 mm) of metal bars were made from Grade 5 titanium alloy with a wire-cut electrical discharge machining (EDM) technique. The shape of the metal bar and measurement method mimicked those in the study of Güth *et al.*<sup>15</sup> The cross-section of the metal bar was a pentagonal shape of 2.5 mm on each side. Two notches were made at the bottom of the bars to increase retention. The coordinates (X, Y, and Z) of two points (A and B) at the end of the metal bars were created from the intersection of planes using a CMM (PMM-C700, Brown and Sharpe, North Kingstown, RI, USA) and used as references. The maximum permissible error for the length measurement ( $MPE_L$ ) of this CMM was  $0.6 + L/600 \mu\text{m}$ , and the reference data were measured with the same method as the test data described below.

Three maxillary dental models were selected from three patients with different arch widths at the intermolar region (small, medium, and large) and were poured with type IV dental stone (Kromotipo4, LOT 0367360108.108, Lascod Spa, Florence, Italy). The different arch widths of the dental models were determined at the mesiopalatal cusp tips of the left and right maxillary first molars in increments of 10 mm difference from small to medium, and medium to large. The 30-, 40-, and 50-mm metal bars were attached to the small, medium, and large models, respectively, using self-cured acrylic resin (Unifast Trad,

LOT 1701172, GC, Tokyo, Japan). The metal bars were placed across the palate with both ends near the mesiopalatal cusp tips of the right and left maxillary first molars (Fig. 1).

The models were installed onto a phantom head before scanning (15 times/group). Three IOSs were compared: TRIOS 3 (TRI) (software version 1.4.7.5, 3Shape Dental Systems, Copenhagen, Denmark), True Definition (TD) (software version 5.1.1, 3M ESPE Dental Products, St. Paul, MN, USA), and Dental Wings (DW) (software version 13.1; Dental Wings INC, Montréal, QC, Canada). Each scanner was calibrated using the manufacturer's guidelines. The scan patterns were also made according to the manufacturer's instructions (Fig. 2). The TRI scanner started from the occlusal surface of the last molar to the ipsilateral canine, then moved in a zigzag motion at the anterior region and continued over the occlusal surface of the opposite posterior teeth, returned from the buccal surface of the contralateral molar to the starting point, and continued along the palatal side. The angle of scanning was 45 - 90 degrees. The TD moved from the occlusal area of the last molar through the incisal edge of the opposite canine, then turned to the palatal side continuously back to the starting molar, and continued along the buccal side to the opposite ca-

nine. After that, the same scan was made on the opposite side. The DW started from the last molar with a zigzag pattern along the arch (move scanner buccal and then palatal). All scans were performed by a well-trained investigator.

The standard tessellation language (STL) data from the scanners were measured by metrology software (Geomagic Control X, 3Dsystem, Cary, NC, USA). Only both ends of the metal bar were scanned with the dental model and used for the measurement and calculation. The planes (Fig. 3A) were constructed by marking the surface on the bar with the best fit algorithm, and the intersections of the planes created points and lines. All data sets were aligned in the same direction, where the base of the bar was set to be parallel to the XY-axis and the length of the bar from the right quadrant to the left quadrant was set to the X-axis (Fig. 3B). Point A (from planes 1, 2, and 4) and point B (from planes 6, 7, and 9) were created and the coordinates of the two points were recorded (Fig. 3C). Vector 1 ( $v_1$ ) and vector 2 ( $v_2$ ) were obtained in the same direction from line A (intersection of planes 1 and 2) and line B (intersection of planes 6, and 7), respectively (Fig. 3D).

The length (L) of the metal bar was calculated from the coordinates of point A ( $X_A, Y_A, Z_A$ ) and point B ( $X_B,$

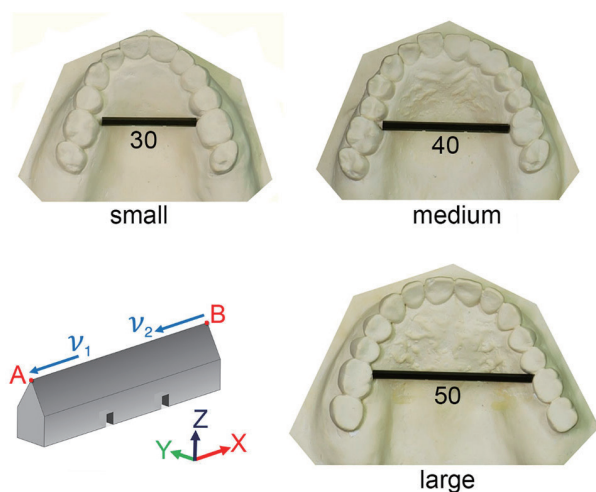


**Fig. 1.** The metal bar with the positions of points A, point B, vector  $v_1$ , vector  $v_2$ , and three sizes of dental models (small, medium, and large) attached with the different lengths of the metal bars (30, 40, and 50 mm).

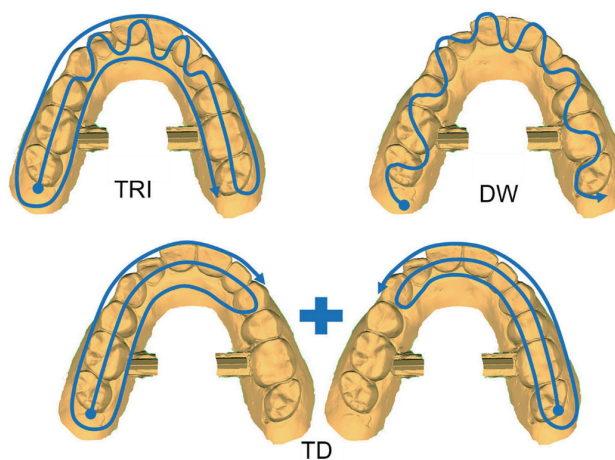


**Fig. 2.** Different scan patterns of the three scanners: TRI = TRIOS 3; DW = Dental Wings, TD = True Definition.

$Y_B, Z_B$ ) as shown in Equation 1:

$$L = \sqrt{(x_B - x_A)^2 + (y_B - y_A)^2 + (z_B - z_A)^2} \quad (1)$$

The deviation of the length ( $\Delta L$ ) was calculated by Equation 2:

$$\Delta L = L_{IOS} - L_{CMM} \quad (2)$$

where  $L_{IOS}$  was the length of the metal bar from the IOS, and  $L_{CMM}$  was the length of metal bar from the CMM.

The accuracy in the length measurement was presented in terms of the percentage of the relative deviation of the trueness ( $RD_T$ ) and relative deviation of the precision ( $RD_P$ ) as shown in Equations 3 and 4:

$$RD_T = \frac{|\Delta L|}{L_{CMM}} \times 100 \quad (3)$$

$$RD_P = \frac{|L_{IOS} - L_{aver}|}{L_{aver}} \times 100 \quad (4)$$

where  $L_{aver}$  was the average length of the metal bar from the IOS.

The coordinates of  $v_1 (xv_1, yv_1, zv_1)$  and  $v_2 (xv_2, yv_2, zv_2)$  on both ends of the bar were used to calculate the angle occurring from the intersection of the two vectors. These vectors would be the same direction if there was no deviation, and the value was going to be zero. The angular deviation of each IOS ( $\alpha_{IOS}$ ) in terms of the trueness was calculated as shown in Equation 5:

$$\alpha_{IOS} = \arccos \frac{xv_1 \cdot xv_2 + yv_1 \cdot yv_2 + zv_1 \cdot zv_2}{\sqrt{xv_1^2 + yv_1^2 + zv_1^2} \cdot \sqrt{xv_2^2 + yv_2^2 + zv_2^2}} \cdot \frac{180}{\pi} \quad (5)$$

The angular deviation in terms of the precision ( $\alpha_p$ ) was calculated as shown in Equation 6:

$$\alpha_p = |\alpha_{IOS} - \alpha_{aver}| \quad (6)$$

where  $\alpha_{aver}$  was the average angle of each IOS.

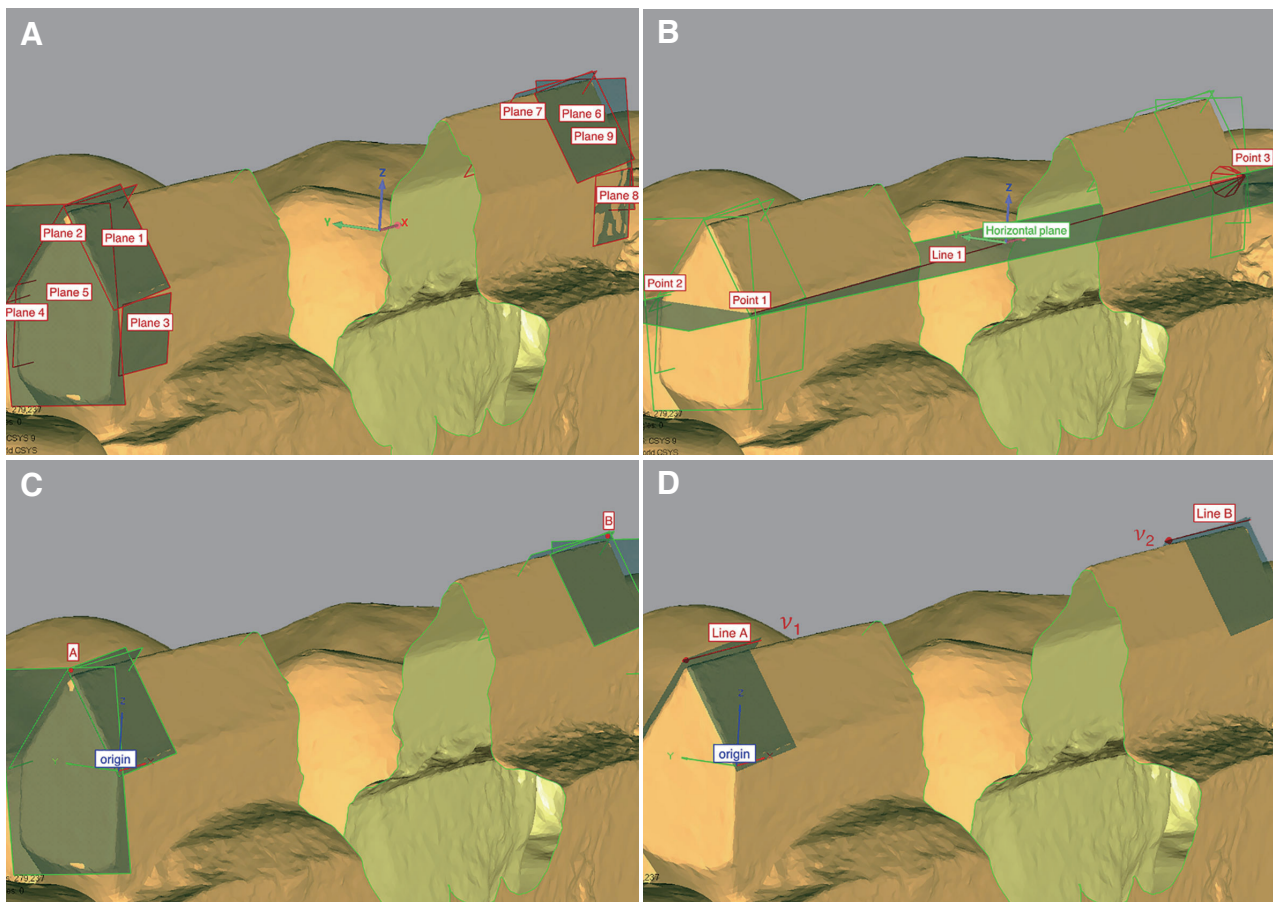


**Fig. 3.** (A) Nine planes (plane 1-9) were created with the best fit algorithm to the metal bar surfaces. (B) Three points (point 1-3) originated from the intersection of the three different planes, and the horizontal plane from these points was set to be parallel to the XY-axis, line 1 from point 1 to point 3 was set to the X-axis. (C) The coordinate of point 1 was set as the origin, and two points (A, B) were created from the intersection of the three different planes. (D) Lines A and B were created from two different planes to obtain the two vectors ( $v_1, v_2$ ) in the same direction.



Normal distribution was evaluated by the Shapiro-Wilk test and the homogeneity of variance was assessed by Levene’s test. Both the trueness and precision were then analyzed with the Kruskal-Wallis test, and followed by Dunn’s post hoc tests for multiple pairwise comparisons. The Bonferroni adjusted p values were selected with the level of significance set at  $P < .05$ .

## RESULTS

The data of the length deviations are shown in Table 1. All groups of the TRI had a negative length deviation, while the DW had a positive length deviation, and the TD showed both positive and negative length deviations depending on the arch size. The statistical data of the relative length deviation and angle deviation in terms of the trueness and precision are presented in Table 2 and Table 3. The Shapiro-Wilk and Levene’s tests revealed that some parameters were not normally distributed and had inhomogeneity of variance. Each scanner presented different ways of deviation. Fig. 4 and Fig. 5 depict the box plots of the relative length and angle deviation in terms of the trueness and precision. The values approaching zero represented high trueness or high precision. The overall mean relative length deviation was between 0.18 -

1.28% for the trueness and 0.06 - 0.38% for the precision. The overall mean angle deviation was between 0.40 - 1.83 degrees for the trueness and 0.15 - 0.50 degrees for the precision.

In terms of trueness, there were significant differences between the scanners. For the small arch, no significant differences were found between the TRI and TD, while the DW revealed the highest deviation (1.28%), which represented the lowest trueness. For the medium arch, the TD had the lowest relative length deviation (0.18%), while the TRI revealed the lowest angle deviation (0.40°), and the DW showed

**Table 1.** Data summary of the length deviation (μm)

|     |        | Mean ± SD | 95% CI     |
|-----|--------|-----------|------------|
| TRI | Small  | -138 ± 36 | -158, -118 |
|     | Medium | -192 ± 66 | -229, -156 |
|     | Large  | -270 ± 37 | -290, -249 |
| TD  | Small  | -50 ± 115 | -114, 14   |
|     | Medium | 58 ± 71   | 19, 97     |
|     | Large  | 119 ± 79  | 75, 163    |
| DW  | Small  | 384 ± 129 | 312, 456   |
|     | Medium | 431 ± 175 | 335, 528   |
|     | Large  | 204 ± 87  | 156, 252   |

SD = standard deviation; CI = confidence interval.

**Table 2.** Relative length deviation in terms of the trueness (RD<sub>T</sub>) and precision (RD<sub>P</sub>)

|             |              | RD <sub>T</sub> (%) |             |             | RD <sub>P</sub> (%) |             |             |
|-------------|--------------|---------------------|-------------|-------------|---------------------|-------------|-------------|
|             |              | TRI                 | TD          | DW          | TRI                 | TD          | DW          |
| Small arch  | Mean (SD)    | 0.46 (0.12)         | 0.33 (0.25) | 1.28 (0.43) | 0.10 (0.06)         | 0.32 (0.20) | 0.36 (0.21) |
|             | Median (IQR) | 0.48 (0.19)         | 0.34 (0.38) | 1.25 (0.86) | 0.09 (0.07)         | 0.25 (0.40) | 0.41 (0.38) |
|             | 95% CI       | 0.39, 0.53          | 0.19, 0.47  | 1.04, 1.52  | 0.06, 0.13          | 0.21, 0.43  | 0.24, 0.48  |
|             | Sig.         | A/a                 | A/a         | B/b         | A/ab                | B/b         | B/b         |
| Medium arch | Mean (SD)    | 0.48 (0.16)         | 0.18 (0.13) | 1.08 (0.44) | 0.14 (0.08)         | 0.14 (0.10) | 0.38 (0.19) |
|             | Median (IQR) | 0.46 (0.27)         | 0.16 (0.23) | 1.17 (0.78) | 0.14 (0.13)         | 0.13 (0.15) | 0.35 (0.30) |
|             | 95% CI       | 0.39, 0.57          | 0.11, 0.26  | 0.84, 1.32  | 0.10, 0.18          | 0.09, 0.20  | 0.27, 0.48  |
|             | Sig.         | B/a                 | A/a         | C/b         | A/b                 | A/ab        | B/b         |
| Large arch  | Mean (SD)    | 0.54 (0.07)         | 0.25 (0.13) | 0.41 (0.17) | 0.06 (0.05)         | 0.12 (0.09) | 0.15 (0.07) |
|             | Median (IQR) | 0.51 (0.10)         | 0.27 (0.21) | 0.45 (0.35) | 0.05 (0.06)         | 0.10 (0.15) | 0.16 (0.12) |
|             | 95% CI       | 0.50, 0.58          | 0.18, 0.33  | 0.31, 0.50  | 0.03, 0.08          | 0.07, 0.17  | 0.11, 0.19  |
|             | Sig.         | B/a                 | A/a         | AB/a        | A/a                 | AB/a        | B/a         |

Sig. = significance; SD = standard deviation; IQR = interquartile range; CI = confidence interval.

The upper-case letters show the significant differences between the scanners.

The lower-case letters show the significant differences within the scanner (between arch widths).

**Table 3.** Angle deviation (°) in terms of trueness ( $\alpha_{ios}$ ) and precision ( $\alpha_p$ )

|             |              | $\alpha_{ios}$ (°) |             |             | $\alpha_p$ (°) |             |             |
|-------------|--------------|--------------------|-------------|-------------|----------------|-------------|-------------|
|             |              | TRI                | TD          | DW          | TRI            | TD          | DW          |
| Small arch  | Mean (SD)    | 0.63 (0.40)        | 0.55 (0.20) | 1.75 (0.54) | 0.32 (0.23)    | 0.16 (0.11) | 0.39 (0.36) |
|             | Median (IQR) | 0.46 (0.71)        | 0.56 (0.32) | 1.77 (0.74) | 0.28 (0.26)    | 0.16 (0.22) | 0.21 (0.70) |
|             | 95% CI       | 0.41, 0.86         | 0.44, 0.66  | 1.45, 2.05  | 0.19, 0.45     | 0.10, 0.22  | 0.19, 0.59  |
|             | Sig.         | A/a                | A/a         | B/b         | A/a            | A/a         | A/a         |
| Medium arch | Mean (SD)    | 0.40 (0.19)        | 0.89 (0.33) | 1.83 (0.63) | 0.15 (0.09)    | 0.28 (0.16) | 0.50 (0.36) |
|             | Median (IQR) | 0.34 (0.35)        | 0.94 (0.67) | 1.80 (1.10) | 0.17 (0.13)    | 0.31 (0.27) | 0.46 (0.47) |
|             | 95% CI       | 0.30, 0.50         | 0.71, 1.07  | 1.48, 2.18  | 0.10, 0.21     | 0.19, 0.37  | 0.29, 0.70  |
|             | Sig.         | A/a                | B/ab        | C/b         | A/a            | AB/a        | B/a         |
| Large arch  | Mean (SD)    | 0.54 (0.22)        | 1.27 (0.34) | 0.98 (0.42) | 0.17 (0.12)    | 0.27 (0.20) | 0.36 (0.19) |
|             | Median (IQR) | 0.48 (0.37)        | 1.37 (0.41) | 0.87 (0.76) | 0.18 (0.16)    | 0.20 (0.33) | 0.37 (0.33) |
|             | 95% CI       | 0.42, 0.66         | 1.08, 1.45  | 0.75, 1.21  | 0.10, 0.24     | 0.16, 0.38  | 0.25, 0.47  |
|             | Sig.         | A/a                | B/b         | B/a         | A/a            | AB/a        | B/a         |

Sig. = significance; SD = standard deviation; IQR = interquartile range; CI = confidence interval. The upper-case letters show the significant differences between the scanners. The lower-case letters show the significant differences within the scanner (between arch widths).

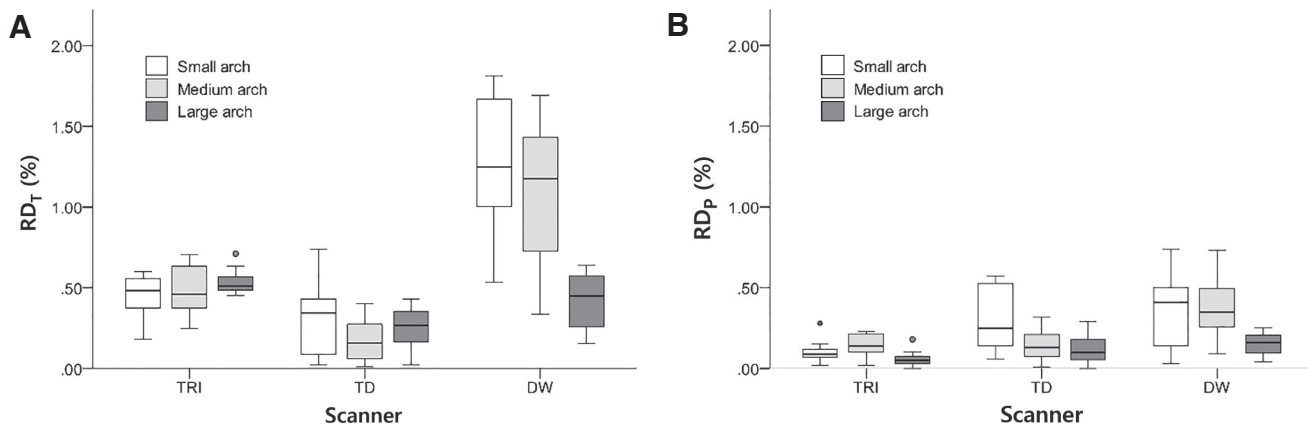


**Fig. 4.** (A) The box plots present the relative length deviation of trueness (RD<sub>T</sub>). (B) The relative length deviation of precision (RD<sub>P</sub>) of the three scanners (TRI = TRIOS 3; TD = True Definition; DW = Dental Wings) in three different arch widths.

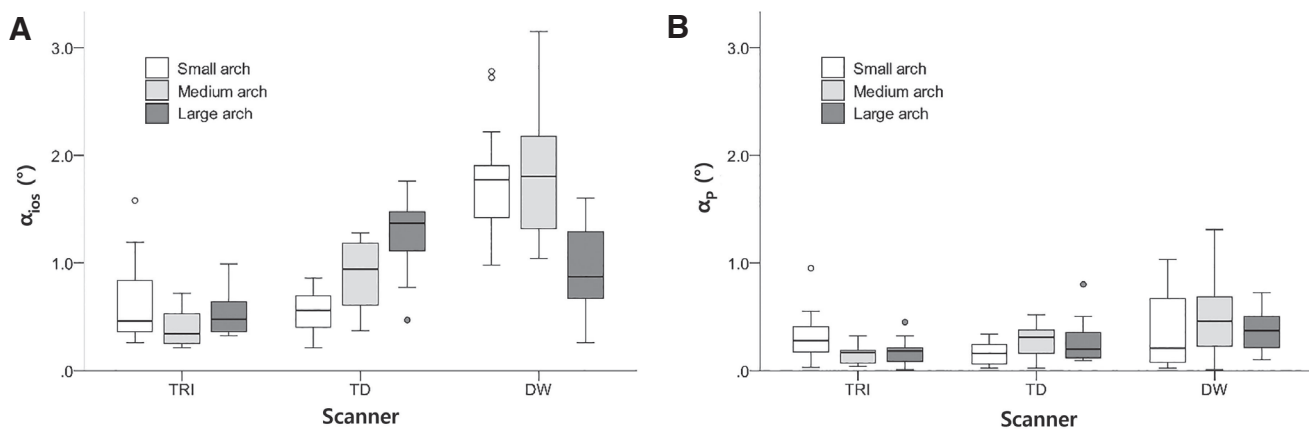


**Fig. 5.** (A) The box plots present the angular deviation in terms of trueness ( $\alpha_{ios}$ ). (B) The angle deviation in terms of precision ( $\alpha_p$ ) of the three scanners (TRI = TRIOS 3; TD = True Definition; DW = Dental Wings) in three different arch widths.

the highest deviation of both parameters. For the large arch, the TD and DW showed no differences in the results of both parameters, while the TRI presented the greatest relative length deviation but had the lowest angular deviation (Fig. 4A and Fig. 5A).

There were significant differences between the arch widths within the TD and DW groups. In the TD group, the highest angular deviation was found in the large arch. In the DW group, the large arch showed the lowest angular and relative length deviation compared to the small and medium arches.

In terms of precision, there were no significant differences between the TRI and TD for both deviations, except the relative length deviation of the small arch where the TRI showed the best precision. Even though all groups of the DW represented the highest deviation, there were no significant differences from the TD group, except the relative length deviation from the medium arch (Fig. 4B and Fig. 5B).

There was no difference in the angular deviation between the width of the arch sizes across all scanners. The relative length deviation of the DW group was significantly lower in the large arch than in the small and medium arches.

## DISCUSSION

Significant differences between the scanners and between the arch widths were found; therefore, the null hypotheses were rejected. Different methods were used for measuring the accuracy of the scanner.<sup>11,23-25</sup> Trueness was probably more difficult to measure than precision because it was necessary to find accurate and reliable reference values for comparison. The superimposition of the 3D scan data with the 3D reference scan by utilizing the best fit algorithm was a widely used method.<sup>6,7,26</sup> However, it would be difficult to find a reliable 3D reference scan, as most of them are questionable. Another method was to measure geometric objects like a sphere or block that would be attached to the teeth while scanning.<sup>15,16</sup> The distance or angle of these objects would be measured with a high accuracy CMM and used as a reference. In the present study, the data sets from a high accuracy CMM with a volumetric probing error of 0.6  $\mu\text{m}$  were used as the references. Although the met-

al bars used as geometric objects in this study were shaped like that in the former study,<sup>15,27</sup> they were prepared with a wire-cut EDM technique creating precision metal bars in three different lengths. This method was appropriate for the preparation of the specimen that required high-profile accuracy and tight dimensional tolerance.<sup>28</sup> Flat and straight planes were created on all sides of the cut. This metal bar design had the advantages of simplifying the determination of the plane and was able to produce the same results. With the intersection of various planes on the metal bar, the coordinate points were created and used for comparing the distances between the test groups and the CMM. The long straight metal bars crossing the quadrant allowed the measurement of the angle deviations from the two vectors in different quadrants. However, this method only measured both ends of the metal bar. Therefore, scanning errors could not be reported on the other part of the dental arch.

The accuracy of the scanner depended on the scanner acquisition and processing software's ability to create realistic 3D virtual models. An important part of obtaining an accurate data set was the resolution of the acquisition of the cameras selected in each scanner.<sup>29,30</sup> The three scanners in this current study used different image capturing technologies and different scanning techniques. The TRI was powered by confocal microscopy technology with ultra-fast scanning. The TD used active wavefront sampling with 3D-in-motion video technology, while the technology of the DW was active triangulation with multiscan imaging. All the scanners had a video sequence data capture mode.<sup>1</sup> When comparing all scanner systems, it was found that the DW had the lowest accuracy in the small and medium arches but presented a result comparable to the other systems in the large arch. Most groups of the TRI showed the lowest angle deviations, while most groups of the TD yielded the lowest relative length deviation. Many previous studies showed different accuracies of the IOSs for a full arch scan.<sup>4,7-12</sup> They tested different IOSs with contrasting methods, so it was difficult to compare this current study with those. However, a former study found that the TD and TRI had the best performance, while the DW showed lower performance.<sup>13</sup> Their findings were

somewhat consistent with the results from the small and medium arches of this study.

In addition, the width of the dental arch changes from birth to middle age. A study reported that the intermolar width could increase from  $30.8 \pm 2.6$  mm at two years of age to  $48.4 \pm 1.6$  mm at 45 years of age in the maxillary arch of females.<sup>31</sup> Due to the various dental arch sizes in each person, three different distances at the mesiopalatal cusp tips of the right and left first maxillary molars were therefore chosen to represent the small, medium, and large arch widths. To compare accuracy with CMM measurements, the geometric objects were inserted in the dental models in which the three metal bars of different lengths were used to match the three arch widths of the dental models, since accurate distances or angles could not be measured directly from the tooth surface. Additionally, measuring long distances was more prone to errors than short distances when using the same tool. However, different arch sizes could be compared without bias from different metal bar lengths using the calculated data from the relative deviations instead of the length deviations. Moreover, the deviations could result in positive or negative values depending on whether they were smaller or larger than the reference. Accurate calculations regardless of the direction of the difference made the comparison reasonable and not affected by uncertain directions. Therefore, a relative deviation with absolute value was used in this study to compare the resulting lengths of the different arch sizes and reported as percentages. In terms of the trueness, the data sets from the CMM were used as the references, while the average values were used as the references in terms of the precision for comparing the length. For the angle deviation, it was measured by the intersection of two vectors ( $v_1, v_2$ ), which was not affected by the different bar lengths. The two vectors were obtained from the two ends of the metal bar, which were independently measured. By forming with the wire-cut EDM technique, the same plane was achieved throughout the metal bar, so the vectors obtained from both ends should be zero degrees if there were no scanning deviations.

Each scanner showed a different way of the length deviation (Table 1). The length measured by the TRI

was shorter than the length obtained by the CMM, which indicated that the dental arch width would be narrower than it should be. On the other hand, the dental arch from the DW was wider than it should have been, while the arch size from the TD appeared to be closer to reality. Güth *et al.*<sup>15</sup> were the first to use a geometrical metal bar in a similar way to this present study. They used a metal bar that was 50.45 mm long and obtained the average length deviation of  $89 \pm 48$   $\mu$ m from the TD scanner, while this current study obtained  $119 \pm 79$   $\mu$ m for a similar length of metal bar (50.14 mm). Another previous study used metal spheres as geometrical objects and measured the distance between the centers of those spheres.<sup>16</sup> With the spherical distance of 45.99 mm at intermolar distances, they reported the absolute length deviation of  $86 \pm 73$   $\mu$ m from the TD,  $97 \pm 77$   $\mu$ m from the TRI, and  $826 \pm 265$   $\mu$ m from the CEREC Omnicam (Dentsply Sirona). In comparing with this study, the absolute length deviation in the large arch was  $126 \pm 67$   $\mu$ m from the TD,  $270 \pm 37$   $\mu$ m from the TRI, and  $204 \pm 87$   $\mu$ m from the DW. A previous study reported that a wider dental arch contributed to the lower precision of the TRI.<sup>22</sup> However, this current study found no differences between the different arch sizes in the TRI group in terms of the precision or trueness. The distortion of the scanned image could be reported as an angle deviation. Measured with a 50.45 mm metal bar length, a previous study found a mean angular deviation of  $0.29 \pm 0.13^\circ$  from the TD.<sup>15</sup> Likewise, another study reported an angular deviation of  $0.46 \pm 0.11^\circ$  from the iTero Element (Align Technology) using a metal bar 55.07 mm long.<sup>27</sup> Most of the data in the current study appeared to have more angular deviations compared to those studies (Table 3).

Previous studies had also shown differences in accuracy based on the size and shape of the scanned object.<sup>26,32</sup> In the case of a full arch scan, the accuracy of all scanners was found to be inferior in the posterior area than the anterior region of the dental arch; consequently, the accuracy would be decreased when increasing the scan area.<sup>6,11,23,26,27</sup> In a larger arch, the scanning area would be greater than a smaller arch. In addition, multiple overlapping scans were performed and combined through stitching the algorithm, as the IOS could not capture the whole



arch with one scan and every stitching process could produce an additional discrepancy. The farther the scanning distance, the more accumulated discrepancies from the scanning. However, only the angle deviation of the TD appeared to be consistent with this phenomenon, while the DW produced impressive results when used in the large arch. It could be said that the width of the dental arch affected the accuracy of the different IOSs in different ways, and this may be why several previous studies with different model sizes showed inconsistent results in the accuracy.

This present study was conducted using three different scan patterns recommended by the manufacturer's guidelines. The scan tracking sometimes could be lost when the range to the object was not fitted. Hence, a scan pattern should begin in the most conventional area in order to prevent the loss of its signal during the scanning process. Manufacturers have also developed different scan patterns and software algorithms to avoid the loss of tracking, and recognition is the main procedure in recording the geometry of the object.<sup>33</sup> However, some scan patterns could affect the accuracy of some scanners in the full arch scan.<sup>30,34</sup>

In addition to different arch widths, the shape and size of teeth also differed from model to model as they were simulated from the actual orals of the patients, and this might influence the scan data set. The effect of different tooth shapes and sizes should be confirmed in subsequent studies. Furthermore, intraoral conditions, such as saliva and limited space, were found to cause an inaccurate scan result.<sup>35,36</sup> Although an attempt was made to mimic a real oral scan by scanning in a phantom head, this *in vitro* study might still avoid factors that would degrade the quality of the scans. In addition, the sample size influenced the value of the standard deviation, which reflected the precision of the scan in this study. Wide standard deviation could result either from a low scanner precision or insufficient sample size, and this was the limitations of this study. Therefore, further studies with an *in vivo* design and larger sample sizes may be required to confirm the results.

The use of the DW scanner in the dental arches with the intermolar width of 30- and 40- mm resulted in greater deviations of the scanned images at the

first molar region than in the dental arch with 50 mm intermolar width. Therefore, there should be some awareness when using DW scanners with small and medium arch widths for full arch scanning. In the large arch where the accuracy was not noticeably different, any of the three scanners could be used. However, the results of this study might not represent the deviation of entire dental arch, but rather indicated scan deviations only at the measurement site. In this current study, only deviations were measured at the area of the first molars. Further study is needed to investigate deviation in the other areas.

## CONCLUSION

Within the limitations of this *in vitro* study, it can be concluded that different dental arch widths and IOSs affect the accuracy of full arch scan at the first molar region. The TD and TRI presented the comparable trueness in the small arch width. Moreover, the TD revealed the lowest relative length deviation across all arch sizes, but its angle deviations increased as the width of the dental arch increased. The DW displayed the lowest accuracy in the small and medium arches but provided a comparable accuracy like other scanners in the large arch.

## REFERENCES

1. Zimmermann M, Mehl A, Mörmann WH, Reich S. Intraoral scanning systems - a current overview. *Int J Comput Dent* 2015;18:101-29.
2. Patzelt SB, Lamprinos C, Stampf S, Att W. The time efficiency of intraoral scanners: an *in vitro* comparative study. *J Am Dent Assoc* 2014;145:542-51.
3. Logozzo S, Zanetti E, Franceschini G, Kilpela A, Makynen A. Recent advances in dental optics - Part I: 3D intraoral scanners for restorative dentistry. *Opt Laser Eng* 2014;54:203-21.
4. Kim RJ, Park JM, Shim JS. Accuracy of 9 intraoral scanners for complete-arch image acquisition: a qualitative and quantitative evaluation. *J Prosthet Dent* 2018;120:895-903.
5. Park JM. Comparative analysis on reproducibility among 5 intraoral scanners: sectional analysis according to restoration type and preparation outline

- form. *J Adv Prosthodont* 2016;8:354-62.
6. Güth JF, Runkel C, Beuer F, Stimmelmayer M, Edelhoff D, Keul C. Accuracy of five intraoral scanners compared to indirect digitalization. *Clin Oral Investig* 2017; 21:1445-55.
  7. Patzelt SB, Emmanouilidi A, Stampf S, Strub JR, Att W. Accuracy of full-arch scans using intraoral scanners. *Clin Oral Investig* 2014;18:1687-94.
  8. Rehmann P, Sichwardt V, Wöstmann B. Intraoral scanning systems: need for maintenance. *Int J Prosthodont* 2017;30:27-9.
  9. Jeong ID, Lee JJ, Jeon JH, Kim JH, Kim HY, Kim WC. Accuracy of complete-arch model using an intraoral video scanner: an in vitro study. *J Prosthet Dent* 2016; 115:755-9.
  10. Malik J, Rodriguez J, Weisbloom M, Petridis H. Comparison of accuracy between a conventional and two digital intraoral impression techniques. *Int J Prosthodont* 2018;31:107-13.
  11. Renne W, Ludlow M, Fryml J, Schurch Z, Mennito A, Kessler R, Lauer A. Evaluation of the accuracy of 7 digital scanners: an in vitro analysis based on 3-dimensional comparisons. *J Prosthet Dent* 2017;118:36-42.
  12. Treesh JC, Liacouras PC, Taft RM, Brooks DI, Raiciulescu S, Ellert DO, Grant GT, Ye L. Complete-arch accuracy of intraoral scanners. *J Prosthet Dent* 2018;120:382-8.
  13. Di Fiore A, Meneghello R, Graiff L, Savio G, Vigolo P, Monaco C, Stellini E. Full arch digital scanning systems performances for implant-supported fixed dental prostheses: a comparative study of 8 intraoral scanners. *J Prosthodont Res* 2019;63:396-403.
  14. Ender A, Mehl A. Accuracy of complete-arch dental impressions: a new method of measuring trueness and precision. *J Prosthet Dent* 2013;109:121-8.
  15. Güth JF, Edelhoff D, Schweiger J, Keul C. A new method for the evaluation of the accuracy of full-arch digital impressions in vitro. *Clin Oral Investig* 2016;20: 1487-94.
  16. Kuhr F, Schmidt A, Rehmann P, Wöstmann B. A new method for assessing the accuracy of full arch impressions in patients. *J Dent* 2016;55:68-74.
  17. Commer P, Bourauel C, Maier K, Jäger A. Construction and testing of a computer-based intraoral laser scanner for determining tooth positions. *Med Eng Phys* 2000;22:625-35.
  18. Chochlidakis KM, Papaspyridakos P, Geminiani A, Chen CJ, Feng IJ, Ercoli C. Digital versus conventional impressions for fixed prosthodontics: a systematic review and meta-analysis. *J Prosthet Dent* 2016;116: 184-90.
  19. Ender A, Zimmermann M, Attin T, Mehl A. In vivo precision of conventional and digital methods for obtaining quadrant dental impressions. *Clin Oral Investig* 2016;20:1495-504.
  20. Ender A, Mehl A. In-vitro evaluation of the accuracy of conventional and digital methods of obtaining full-arch dental impressions. *Quintessence Int* 2015;46:9-17.
  21. Giménez B, Özcan M, Martínez-Rus F, Pradies G. Accuracy of a digital impression system based on parallel confocal laser technology for implants with consideration of operator experience and implant angulation and depth. *Int J Oral Maxillofac Implants* 2014;29:853-62.
  22. Gan N, Xiong Y, Jiao T. Accuracy of intraoral digital impressions for whole upper jaws, including full dentitions and palatal soft tissues. *PLoS One* 2016;11: e0158800.
  23. Nedelcu RG, Persson AS. Scanning accuracy and precision in 4 intraoral scanners: an in vitro comparison based on 3-dimensional analysis. *J Prosthet Dent* 2014;112:1461-71.
  24. Lim JH, Park JM, Kim M, Heo SJ, Myung JY. Comparison of digital intraoral scanner reproducibility and image trueness considering repetitive experience. *J Prosthet Dent* 2018;119:225-32.
  25. Stimmelmayer M, Güth JF, Erdelt K, Edelhoff D, Beuer F. Digital evaluation of the reproducibility of implant scanbody fit-an in vitro study. *Clin Oral Investig* 2012; 16:851-6.
  26. Fukazawa S, Odaira C, Kondo H. Investigation of accuracy and reproducibility of abutment position by intraoral scanners. *J Prosthodont Res* 2017;61:450-9.
  27. Keul C, Güth JF. Accuracy of full-arch digital impressions: an in vitro and in vivo comparison. *Clin Oral Investig* 2020;24:735-45.
  28. Pramanik A, Basak AK, Littlefair G, Debnath S, Prakash C, Singh MA, Marla D, Singh RK. Methods and variables in electrical discharge machining of titanium alloy - a review. *Heliyon* 2020;6:e05554.
  29. Ting-Shu S, Jian S. Intraoral digital impression tech-

- nique: a review. *J Prosthodont* 2015;24:313-21.
30. Ender A, Mehl A. Influence of scanning strategies on the accuracy of digital intraoral scanning systems. *Int J Comput Dent* 2013;16:11-21.
  31. Bishara SE, Jakobsen JR, Treder J, Nowak A. Arch width changes from 6 weeks to 45 years of age. *Am J Orthod Dentofacial Orthop* 1997;111:401-9.
  32. Park JM, Kim RJ, Lee KW. Comparative reproducibility analysis of 6 intraoral scanners used on complex intracoronal preparations. *J Prosthet Dent* 2020;123:113-20.
  33. Richert R, Goujat A, Venet L, Viguie G, Viennot S, Robinson P, Farges JC, Fages M, Ducret M. Intraoral scanner technologies: a review to make a successful impression. *J Healthc Eng* 2017;2017:8427595.
  34. Müller P, Ender A, Joda T, Katsoulis J. Impact of digital intraoral scan strategies on the impression accuracy using the TRIOS Pod scanner. *Quintessence Int* 2016;47:343-9.
  35. Ender A, Attin T, Mehl A. In vivo precision of conventional and digital methods of obtaining complete-arch dental impressions. *J Prosthet Dent* 2016;115:313-20.
  36. Gedrimiene A, Adaskevicius R, Rutkunas V. Accuracy of digital and conventional dental implant impressions for fixed partial dentures: a comparative clinical study. *J Adv Prosthodont* 2019;11:271-9.